Research Report

2003-16

Performance Evaluation of An Axial Flux Consequent Pole PM Motor Using Finite Element Analysis

M. Aydin, S. Huang*, T.A. Lipo

Electrical and Computer Engineering Dept.
University of Wisconsin-Madison
1415 Engineering Dr.
Madison, WI 53706-1691, USA

*Department of Automation
Shanghai University
149 Yan-Chang Road
Shanghai, 200072, P.R.China

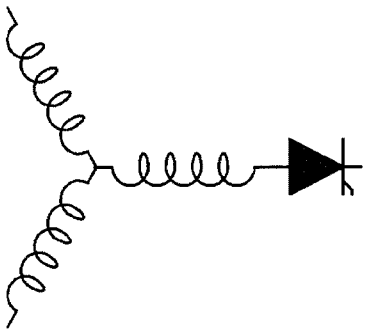

Wisconsin
Electric
Machines &
Power
Electronics
Consortium

University of Wisconsin-Madison
College of Engineering
Wisconsin Power Electronics Research Center
2559D Engineering Hall
1415 Engineering Drive
Madison WI 53706-1691

Performance Evaluation of An Axial Flux Consequent Pole PM Motor Using Finite Element Analysis

Metin Aydin[1], *Student Member, IEEE* Surong Huang [2], *Member, IEEE* Thomas A. Lipo[1], *Fellow, IEEE*

[1]Electrical and Computer Engineering Department
University of Wisconsin-Madison
1415 Engineering Drive
Madison, WI 53706-1691, U.S.A

[2]Department of Automation
Shanghai University
149 Yan-Chang Road
Shanghai, 200072, P.R. CHINA

***Abstract* – Performance evaluation of an axial flux surface mounted permanent magnet (PM) field controlled TORUS type (FCT) disc machine is presented in this paper. This new machine is an axial flux configuration with true field weakening capability since the flux is controlled by the DC field winding rather than opposing the magnets. Structure and operating principles are summarized in the first section. Next, 3D Finite Element Analysis (FEA) including no-load and on-load characteristics and back EMF variation for various armature currents and DC field current are explored. Furthermore, torque characteristics of the FCT machine for different field currents are explored. Minimization of cogging torque calculations and the effect of skewing the magnets are also examined.**

I. INTRODUCTION

Excitation control of synchronous generators to regulate voltage, variable speed and constant power mode operation in DC and synchronous motor above base speed can easily be accomplished by controlling the field current. However, in PM machines, there exists a fixed magnetic excitation which limits the maximum speed of the drive and restricts the development and application of the PM machines, such as the drive's constant power operating mode and hence the maximum speed of the machine. Thus it poses a significant limitation for both radial and axial flux PM machines. In the conventional approach, drives are controlled to operate at constant volts per hertz operation up to base speed and constant voltage operation above base speed to reduce the field so as to overcome this problem. In order to reduce the air-gap flux at high speeds, vector control techniques are used and a negative component of d-axis current is injected into the stator winding. If a large negative d-axis component of current is applied, the magnets may be made to operate in the irreversible demagnetization region and after the current is removed the magnets may not be able to return to their original operating point. In addition this method increases the conduction losses in the stator winding. Hence, this approach results in reduced torque and efficiency of the machine. Furthermore, this mode of operation affects the constant power region of the machine since the demagnetizing current limits the constant power region.

Authors would like to thank Enova Systems, Wisconsin Electrical Machines and Power Electronics Consortium (WEMPEC) and National Science Foundation of China (#50277024) for their support of this research presented in this paper.

To achieve field weakening or control in PM machines by eliminating the effects of d-axis current injection have been of great interest in the literature. New alternative topologies with field weakening or hybrid excitation introduced in the literature so far to eliminate this problem are from a machine perspective [1-9] and meant especially for radial flux machines. However, there exists no axial flux machine with true field weakening capability in the literature. In our previous work, a new consequent pole field controlled axial flux surface mounted PM machine has been proposed not only to overcome this drawback but also to improve the overall features of PM machines [10]. It also allows one to use the machine for applications that has space constraints. This new field controlled PM machine has a wide variety of application scope such as electric propulsion motors requiring constant power operation in the wide speed range and vehicle starter/generator requiring constant back-emf operation in the wide speed range. Airgap flux control allows many advantages such as simple flux control, no demagnetization risk of the magnets, voltage control of generator operation, and also extends the constant power region operation. The major purpose of this paper is to evaluate the performance and provide some three-dimensional (3D) FEA results as well as a suitable test set up for the proposed PM machine.

In this paper, first the structure of the new axial flux PM machine, its operating principles and the concept of airgap flux control are summarized. Then 3D FEA including no-load and on-load characteristics, back EMF evaluation, static torque and torque per ampere characteristics are examined. In order to evaluate the axial flux machine topology an experimental system set-up is devised and discussed in the final section of the paper.

II. STRUCTURE OF A NEW AXIAL FLUX PM MACHINE

Figure 1 shows the FCT machine structure. The stator structure seen in Figure 2 (a) is formed by two strip wound or tape wound stator rings, circumferentially wound DC field winding and two sets of 3 phase AC winding. The stator core is divided into two sections in order to insert the DC field winding, which makes it possible to alter the net air gap flux. The stator core has also slots to accommodate the two sets of 3 phase AC windings which may be connected in either series or parallel.

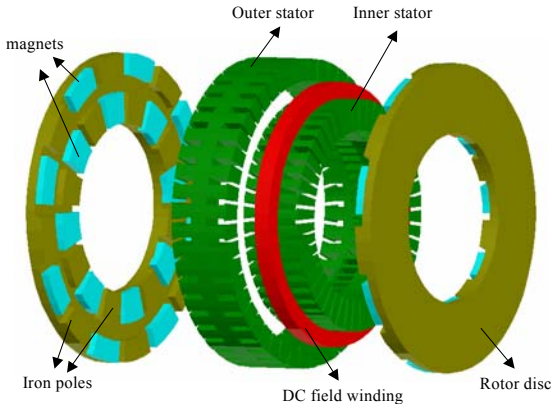

Fig. 1. 3D view of the new axial flux surface mounted field controlled PM machine without 3 phase AC winding

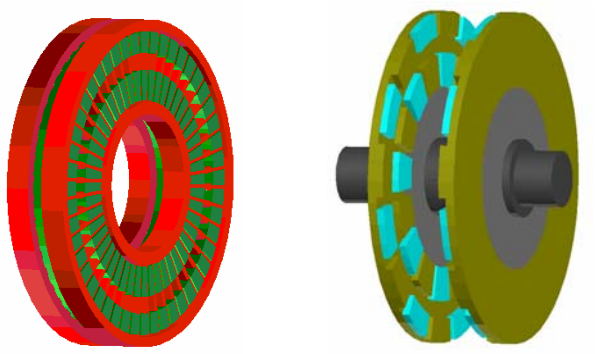

(a) (b)

Fig. 2. 3D view of the stator (a) and rotor (b) structures of the FCT machine

Similar to the stator structure, the rotor is divided into two parts as shown in Figure 2 (b). The outer section of the rotor has magnets with same direction of magnetization (say North) and is called the N-pole side. The inner section of the rotor has the opposite polarity of magnets (say South) and are called S-pole magnets. In other words, the permanent magnets which are mounted on every other pole in the outer section are magnetized such that the N-poles face the air gap. The non-magnet poles are salient poles of iron core. Likewise, the S-pole side magnets on the inner section of the rotor are magnetized in such a manner that S-poles face the air gap. The S-pole magnets are again located on every other pole and aligned with the N-pole side magnets.

III. Principle of Operation and Airgap Flux Control

The basic control principle of the machine is illustrated in Figure 3 which shows the directions of the flux above the magnets, iron pieces and machine rotors with no field current (a), with positive (b) and with negative field current (c) cases respectively. Stator rings are eliminated in order to illustrate the machine principle explicitly. When a positive current is applied to the field winding, average airgap flux is reduced since the flux directions above the magnets and iron pieces are opposite. As the direction of the field current is changed, the flux direction above the iron pieces changes and the flux created by the field winding is added to the magnet flux. In other words, excitation of the DC field winding of one polarity tends to increase the flux on both inner and outer portions of the rotor pole thus strengthening the magnetic field and increasing the flux linking the stator armature windings. Excitation of the field winding with the opposite polarity will decrease the flux in the consequent poles in both inner and outer portions of the rotor disc, thus achieving field weakening.

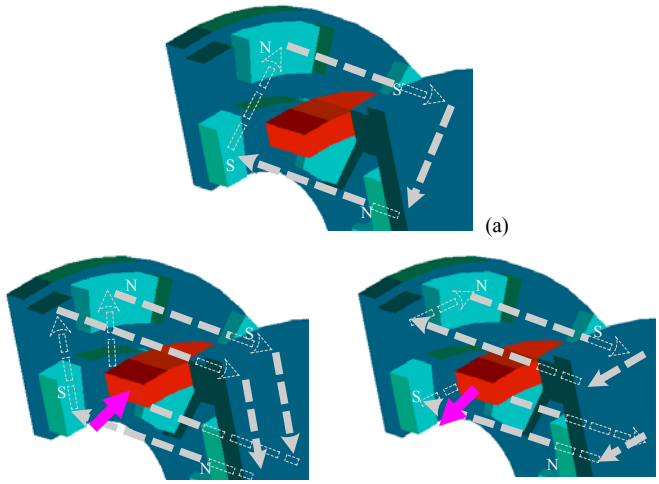

Fig. 3 Operating principle of the FCT machine showing the magnet created and field winding created flux components: (a) No DC field current, (b) negative DC field current and (c) positive DC field current

Figure 4 shows the 3-dimensional flux density distribution over one pole section for three different cases of the DC field current (0 Aturns, +1200 Aturns and –1200 Aturns) and proves the principles of the airgap flux control. As can be noted from the plots, the flux density magnitude and directions on the iron poles indicate that the flux over one pole can be weakened or strengthened depending on the direction of the DC current. Since the magnet flux does not change with the DC field current, the resultant airgap flux which is the superposition of the PM flux and iron flux alters with the field current direction and magnitude resulting in weakened or strengthened flux in the airgap. The slotting effects of the machine stator are also monitored from the three figures.

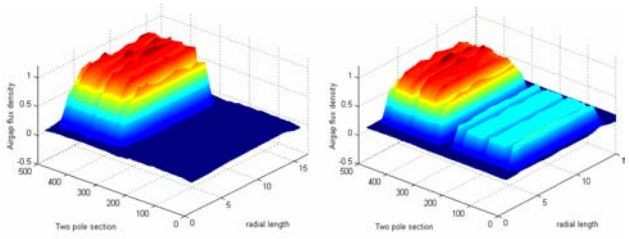

(a) (b)

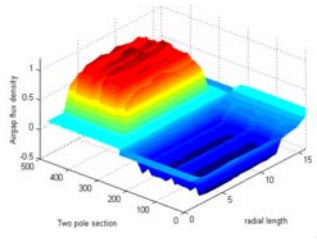

(c)

Fig. 4 Airgap flux density distribution for different values of the DC field current over two poles (a) 0 Aturns, (b) +1200 Aturns, (c) –1200 Aturns

IV. Evaluation of Machine Characteristics Using 3D Finite Element Analysis

FEM can accurately analyze the models involving permanent magnets of any shape and material. There is no need to calculate the reluctances, inductances and sometimes torques using circuit type analytical methods since these values can simply be extracted from the finite element analysis. One important advantage of using FEM over analytical approach is the ability to calculate the torque variations such as cogging torque, ripple torque and resultant torque with changes in rotor position. Different FCT machine models are used in the no-load and on-load analyses and the results are obtained for various aims such as control range, cogging torque, torque per ampere and back EMF. Maxwell 3D© software package by Ansoft was used in the analysis of FCT machine [11].

A. FEA Model of the Machine

The simplified machine model is shown in Figure 5. In order to simplify the machine model and reduce the calculation time, one fourth of the machine is analyzed. Optimization study revealed that the machine efficiency has a maximum for 16 poles which was chosen as the machine pole number. Slot per pole per phase is chosen as one because of the space constraint. The end winding effect was neglected in the model because of the complexity needed to create the model and the computation time to analyze it in 3D. The magnet pole arc was chosen to be 0.82 after detailed investigation of the magnet flux leakage between poles.

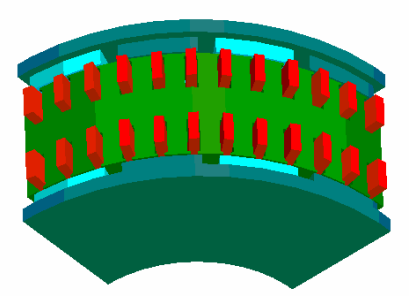

Fig. 5. 3D FEA model of the FCT machine

B. No Load Characteristics

Figure 6 (a) illustrates the flux per pole obtained from the 3D FEA analysis. Each component of the airgap flux corresponding to airgap flux in front of the magnet piece, iron pole and the resultant flux over one pole is calculated for various values of the DC field current. The resultant flux over one pole coming from both sources is also calculated and plotted in Fig. 6 (b) as the DC current varies. As can be seen from the airgap flux components, the resultant airgap flux can be weakened or strengthened with respect to zero DC field current case. With the variation of the rated value of DC field current, the airgap flux control range at no load becomes roughly 87%.

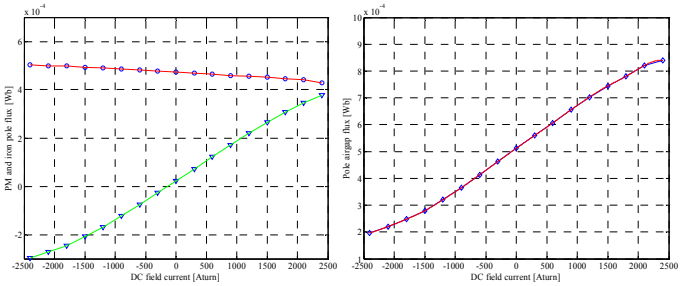

(a) (b)

Fig. 6 Magnet and iron pole flux (a) and resultant airgap flux over one pole as a function of DC field current (No load)

C. Evaluation of Back EMF

Time performance of back EMF can be evaluated by the space derivative of the flux linked with windings and can be expressed as

$$e(t) = -\frac{d\psi(\theta)}{d\theta}\frac{d\theta}{dt} = -\frac{d\psi}{d\theta}\omega_r \qquad (1)$$

where e is the phase airgap back EMF, ψ is the airgap flux linkage per phase, θ is the rotor position and ω_r is the angular speed of the rotor. The back EMF is obtained by using numerical derivation of the linked flux. The flux linked for a given position of the rotor can be expressed as

$$\psi(\theta) = \frac{1}{S}\int A.dS \qquad (2)$$

where S is the cross sectional area of the winding. By changing the rotor position in small steps different sets of rotor position-linked flux values are obtained. Using numerical interpolation or numerical derivation, the behavior of the back EMF can be found easily. It should be mentioned that cogging torque evaluation and back EMF evaluation can be accomplished together and no additional FEA model is required for back EMF or cogging torque analysis.

Rotor position-linked flux values has been obtained using 3D FEA for different positive and negative DC field current values and shown in Figure 7. One way to calculate the back

EMF is to do the calculation via direct numerical derivation. However, the accuracy of this method is poor since a small number of points for each rotor position are calculated. If the flux varies in between two rotor positions under consideration, the significant numerical errors will be produced. Therefore, linked flux for FCT machine was interpolated using cubic splines. In order to obtain the variation of back EMF airgap flux was measured for different positions and these flux values were interpolated by cubic splines. Taking the numerical derivative of this waveform will result in back EMF variation of the machine which was displayed in Figure 8 for various values of the DC field current. It is obvious that the machine back EMF can be easily increased or reduced by applying positive or negative current to the field coil. This easy field control by field coil is the most important feature of the FCT machine.

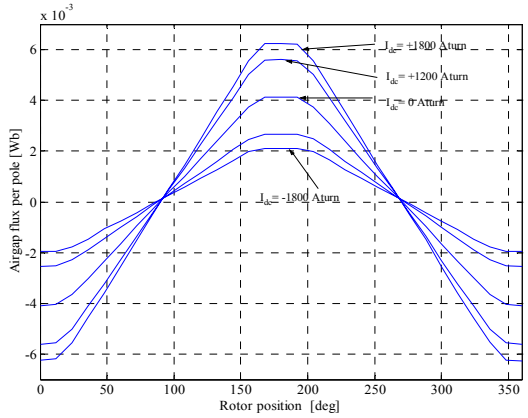

Fig. 7. Airgap flux (per turn per rpm) variation of the FCT machine for different DC field currents

It should be mentioned that the back EMF shape of a machine is closely related to the flux density waveform. Flux density waveform has a direct effect on ripple torque. The reason for this behavior is that the torque is proportional to the product of the current and the flux density (or back EMF waveform) and therefore the ripple in the back EMF will show up directly in the torque waveform.

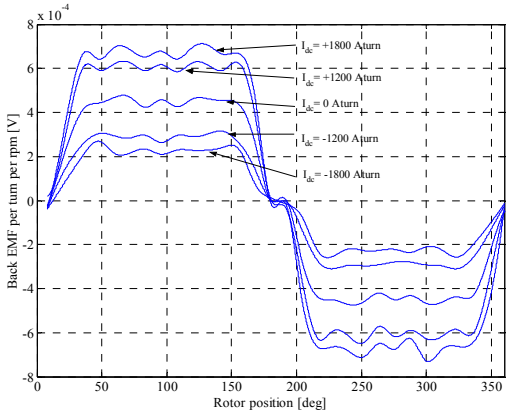

Fig. 8. Back EMF (per turn per rpm) variation of the FCT machine for different DC field currents

D. On Load and Torque Characteristics of the FCT Machine

Figure 9 shows the torque vs. armature current for motoring operation. As one sees from these characteristics, machine torque increases as the armature current is increased. Torque variation against armature current for a given DC field current is close to linear for small values of field current. Saturation effect, which is caused by higher flux density in the machine stator and teeth, can be seen for higher values of field and armature currents.

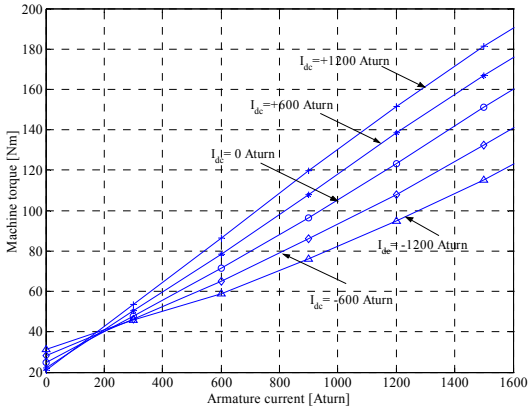

Fig. 9 Machine torque for various values of armature and field currents

Analyses of the FCT machine torque examining the torque for various field currents, peak torque at rated stator current conditions and cogging torque minimization by using magnet skew technique were also accomplished in this section. Figure 10 shows the resultant torque variation of the machine when the stator windings are supplied with currents as the rotor rotates with a constant power angle.

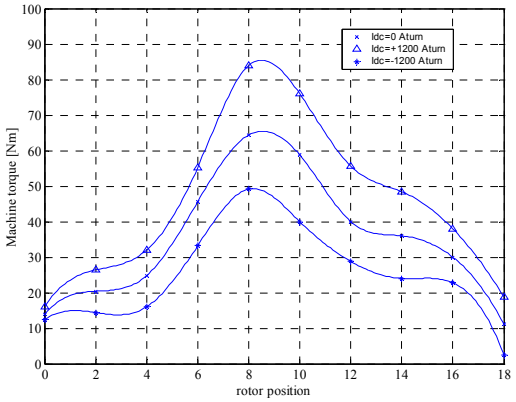

Fig. 10. Static torque characteristics of the FCT machine for different field current values at rated conditions

It shows the static torque characteristic of the machine at rated armature current and field current conditions. The torque variation is obtained for different field current cases over one rotor pole. This result implies that the machine

torque can be controlled by nearly 51% with respect to no DC current case.

E. Cogging Torque Computations

Cogging torque is one of the most important sources of torque pulsating in PM machines and can be minimized using many techniques [12-13]. Same minimization techniques can be applied to axial flux machines as well [14]. The method involving the skewed magnets is the only technique which was used to reduce the cogging torque component of the FCT machine simply because of the fact that it is an uncomplicated cost effective process compared to some other techniques used in axial flux PM machines. Optimization work is accomplished using 3D FEA in order to find out the optimum skew angle. The cogging torque variation of the FCT machine for different skew angles and peak torque variation as a function of skew angle is displayed in Figures 11 and 12 respectively.

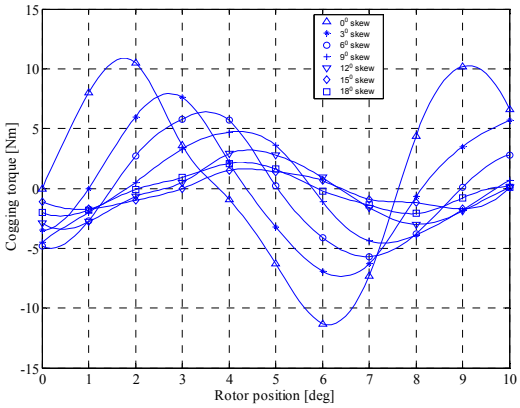

Fig. 11. Peak cogging torque variation for different magnet skew angles

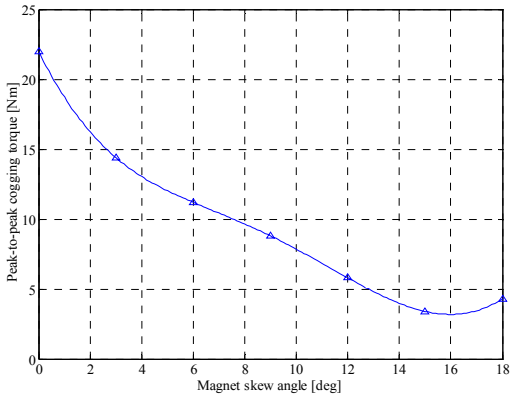

Fig. 12. Peak to peak cogging torque for the FCT machine for different skew angles

The figures illustrate that the cogging torque has a peak value of 11 Nm for the non-skewed magnet case, which is about 23% of the machine rated torque. As the magnets are skewed by steps of 3 degrees, the peak cogging torque starts to go down and reaches a minimum value at 15 degrees. Skew angle of 15 degrees allows minimum cogging torque of nearly 3 Nm. In other words, 15 degree skewing results in a peak cogging torque of 3 Nm which is 6% of the rated torque and 73% less than the cogging torque calculated with no skewing. After this critical value, the trend of the cogging torque value reverses. Thus, if the machine is designed for 15 degree skew, the cogging torque component is minimized for the designed power range and pole number.

V. System Set-up and Control of the Machine

In order to verify the performance of the FCT machine, a 3-phase voltage source power converter has been fabricated. The converter consists of a diode bridge at the front end and regular IGBT based PWM inverter for driving the machine. Testing system schematic used in the experimental work is illustrated in Figure 9.

As can be seen from the figure, the drive system includes the FCT machine prototype, converter for the 3-phase AC winding, a DC Power supply for the DC field winding and a DSP based controller. A separate DC power supply is used for the field winding to simplify the control and converter. A 20 HP, 2000 rpm DC machine which is operated as a generator is initially used as a variable load for the FCT motor. An adjustable resistive load bank is connected to the armature winding of the DC machine. The field winding of the DC machine is fed by another DC power supply. In this set-up, DC machine can also be used as a motor to drive the FCT machine in order to obtain the open circuit back EMF waveform. A torque transducer (TT) can be used for measuring the output torque of the FCT machine. The TT is placed in between the FCT machine and DC machine.

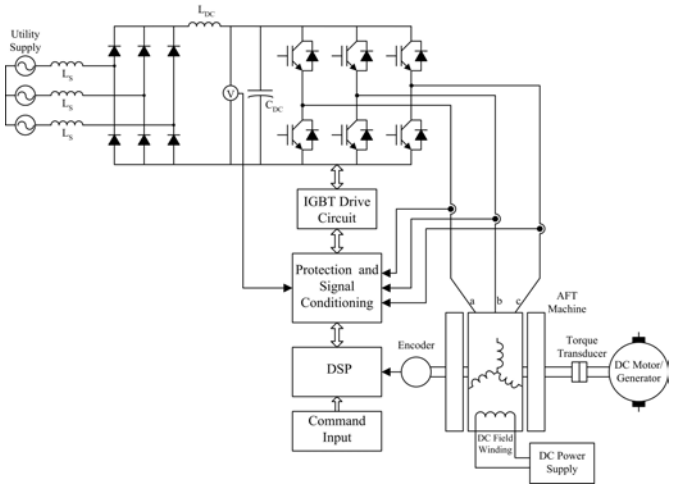

Fig. 13. Experimental system set-up of the field controlled axial flux PM machine

The torque versus rotor position, back EMF and pole flux variation for various DC field currents will be obtained in the experimental analysis and compared with the finite element results. An indexing machine or dividing head will be used to stall the rotor so that the static torque values can be recorded at different positions. In addition, flux linkage and back EMF measurements will be accomplished in the experimental study.

VI. Conclusions

Performance evaluation of the new FCT machine capable of field control has been presented in this paper. 3D finite element analysis of the topology is illustrated in detail. No-load and on-load characteristics of the machine for various armature currents and DC field currents are explored. Flux linkage and back EMF variation of the machine are calculated using 3D FEA and it was found out that the control using field winding is very simple and a wide range of control can be accomplished. Furthermore, torque characteristics of the FCT machine for different field currents are also explored. The effect of skewing the magnets is also accomplished and it was found out that the cogging torque can be minimized by simply skewing the magnet pieces. The experimental system set-up was also introduced and experimental results will be presented in future papers.

References

[1] Y. Li and T. A. Lipo, "A doubly salient permanent magnet motor capable of field weakening", *IEEE Power Electronics Specialists Conference*, 1995; pp.565-571.

[2] B. J. Chalmers, R. Akmese, L. Musaba, "Design and field-weakening performance of permanent-magnet/reluctance motor with two-part rotor", *IEE proceedings*, Vol.145, No.2, March 1998, pp.133-139.

[3] L. Xu, L. Ye, L. Zhen and A. El-Antably, "A new design concept of permanent magnet machine for flux weakening operation", *IEEE Transactions on Industry Applications*, Vol. 31, No. 2, March/April 1995, pp.373-378.

[4] J.A. Tapia, F. Leonardi and T. A. Lipo, "Consequent pole PM machine with field weakening capability", *IEEE International Conference on Electrical Machines and Drives*, Boston, 2001, pp.126-131.

[5] F. Liang, J. M. Miller, X.Y. Xu, "Hybrid permanent magnet /synchronous machines," Mar.19, 2002, US Patent 6,359,366.

[6] A.Detela, "Hybrid synchronous machine with transverse magnetic flux," Jan. 27, 1998, US Patent 5,712,521.

[7] Shah; Manoj Ramprasad, Kliman; Gerald Burt, "Hybrid synchronous machines comprising permanent magnets and excitation windings in cylindrical element slots," Jan. 21, 2003, US Patent, 6,509,664.

[8] Y. Amara, E. Hoang, M. Gabsi, M. Lecrivain, A.H.B. Ahmed, S, Derou, "Measured performances of a new hybrid excitation synchronous machine," EPE Journal (European Power Electronics and Drives Journal), vol.12, pp.42-50, Sept./Oct./Nov. 2002.

[9] Y. Amara, J. Lucidarme, M. Gabsi, M. Lecrivain, A.H.B. Ahmed, A.D. Akemakou, "A New Topology of Hybrid Synchronous Machine," IEEE Transactions on Industry Applications, vol.37, pp.1273-12815. Sept./Oct. 2001.

[10] M. Aydin, S. Huang and T. A. Lipo, "A new axial flux surface mounted permanent magnet machine capable of field control", *IEEE Industry Applications Annual Meeting*, Oct 2002, pp. 1250-1257.

[11] Maxwell 3D Users Manual, Pittsburg 2002.

[12] T. Li and G Slemon, "Reduction of cogging torque in permanent magnet motors", IEEE Transactions on Magnetics, Vol. 24, No. 6, Nov 1988, pp. 2901-2903.

[13] T. M. Jahns, W. L. Soong, "Pulsating torque minimization techniques for permanent magnet AC motor drives-a review", IEEE Transaction on Industrial Electronics, Vol.43, No.2, 1996, pp. 321-330.

[14] M. Aydin, "Axial flux surface mounted PM machines for traction drive applications", PhD Preliminary Report, University of Wisconsin-Madison, 2002.